J Mater Sci: Mater Med (2009) 20:145–155
DOI 10.1007/s10856-008-3561-8

Effect of the hard segment chemistry and structure on the thermal and mechanical properties of novel biomedical segmented poly(esterurethanes)

P. C. Caracciolo · F. Buffa · G. A. Abraham

Received: 9 June 2008 / Accepted: 25 July 2008 / Published online: 14 August 2008

Abstract Two series of biomedical segmented polyurethanes (SPU) based on poly(ε-caprolactone) diol (PCL diol), 1,6-hexamethylene diisocyanate (HDI) or L-lysine methyl ester diisocyanate (LDI) and three novel chain extenders, were synthesized and characterized. Chain extenders containing urea groups or an aromatic amino-acid derivative were incorporated in the SPU formulation to strengthen the hard segment interactions through either bidentate hydrogen bonding or π-stacking interactions, respectively. By varying the composition of the hard segment (diisocyanate and chain extender), its structure was varied to investigate the structure-property relationships. The different chemical composition and symmetry of hard segment modulated the phase separation of soft and hard domains, as demonstrated by the thermal behavior. Hard segment association was more enhanced by using a combination of symmetric diisocyanate and urea-diol chain extenders. The hard segment cohesion had an important effect on the observed mechanical behavior. Polyurethanes synthesized using HDI (Series H) were stronger than those obtained using LDI (Series L). The latter SPU exhibited no tendency to undergo cold-drawing and the lowest ultimate properties. Incorporation of the aromatic chain extender produced opposite effects, resulting in polyurethanes with the highest elongation and tearing energy (Series H) and the lowest strain at break (Series L). Since the synthesized biodegradable SPU possess a range of thermal and mechanical properties, these materials may hold potential for use in soft tissue engineering scaffold applications.

P. C. Caracciolo · F. Buffa · G. A. Abraham (✉)
Instituto de Investigaciones en Ciencia y Tecnología de Materiales, INTEMA (UNMdP-CONICET), Av. Juan B. Justo 4302, B7608FDQ Mar del Plata, Argentina
e-mail: gabraham@fi.mdp.edu.ar

1 Introduction

To date, most of the biodegradable materials available for use in tissue engineering are hard, brittle substances best suited to bone and hard tissue applications. Several tissues that need to be replaced or regenerated, however, are soft tissues that require large elasticity. Thus, there is a need for synthetic degradable materials that exhibit the properties of elastic recoil and malleability. Polyurethanes comprise a broad family of materials, including segmented polyurethane elastomers (SPU), rigid thermoset networks, adhesives, and flexible elastomeric foams [1, 2]. In recent years, a significant number of novel biocompatible and biodegradable SPU elastomers have been investigated. Although their potential for tissue regeneration and drug delivery has not been evaluated in vivo, these polymers are promising for applications in biomedical devices [2–5].

The highly variable chemistry of SPU allows the preparation of materials with a wide range of physico-chemical, mechanical, and biological properties that can be achieved through the appropriate selection of monomers. Many applications of SPU in the tissue engineering field, such as cardiovascular tissue engineering [6–8], musculoskeletal applications (anterior cruciate ligament [9], knee joint meniscus [10, 11], bone tissue engineering [12, 13], smooth muscle cell constructs for contractile muscle [14, 15]), and nerve regeneration [16], have been recently evaluated.

The unique and versatile properties of SPU elastomers are directly related to their two-phase microstructure, with hard domains acting as thermally reversible crosslinking points, and soft domains constituting the flexible segments [1, 17]. Polyester soft segments are commonly used to provide hydrolytically labile segments. When appropriately designed, chain extenders are able to impart specific properties to the material. For example, chain extenders

containing easily hydrolyzable linkages increase the degradation rate of polyurethanes [18, 19]. Moreover, chain extenders can also be designed to promote highly ordered microphase-separated hard domains. Thus, the incorporation of urea linkages strengthens hard segment interactions through bidentate hydrogen bonding of urea groups in adjacent chains [12], and the presence of aromatic groups also strengthens inter-chain hard segment attractions due to π-bond stacking among adjacent aromatic rings of symmetrical structure [1]. The cooperative character of all interactions within the hard segment domains determines the thermal and mechanical behavior.

Biomedical segmented poly(esterurethanes) and poly(esterurethane urea)s based on poly(ε-caprolactone) (PCL) and aliphatic diisocyanates, such as 1,4-butane diisocyanate (BDI), hexamethylene diisocyanate (HDI), L-lysine ethyl (or methyl) ester diisocyanate (LDI), 1,4-*trans*-cyclohexane diisocyanate (CHDI) and isophorone diisocyanate (IPDI), have been synthesized using a broad variety of chain extenders. Several examples of chain extenders reported in the literature include short-chain diamines [20, 21], amino-acids or amino-acid derivatives [5, 18, 22], short-chain diols [10, 11, 23], amino-diols [23], short-chain diester-diols [19] and diurea-diphenols based on tyramine or tyrosine [12, 13].

In a previous paper we reported on the preparation, physicochemical characterization, and in vitro biological properties of two aliphatic segmented poly(esterurethane urea)s based on PCL, HDI and two novel urea-diol chain extenders [24]. In the present work, two series of PCL-based SPU are synthesized from either HDI or LDI, and aliphatic or aromatic chain extenders containing urea or ester groups, respectively. The effect of the hard segment chemistry and structure on the thermal and mechanical properties of these biomedical SPU is investigated and discussed.

2 Materials and methods

2.1 Materials

ε-caprolactone, ethylene glycol (EG), triethylene glycol (TEG), 2-aminoethanol (AE), 3-(4-hydroxyphenyl)propionic acid (desaminotyrosine, DAT), *p*-toluene sulfonic acid (*p*-TsOH), HDI, and *N*,*N*-dimethylacetamide (DMAc) were obtained from Aldrich. EG, TEG and *p*-TsOH were dried under vacuum at 60°C for 24 h prior to use, DMAc was kept over molecular sieves (4 Å) and distilled under vacuum, and the rest of the reagents were used as received. LDI was kindly donated by Kyowa Hakko Kogyo Co., Ltd, Japan. Dibutyltin dilaurate (Fluka) was used as catalyst.

2.2 Synthesis of macrodiol and chain extenders

PCL diol was synthesized by ring-opening polymerization of ε-caprolactone initiated by TEG. The number-average molecular weight (M_n) determined by end-group titration was 2,250. Two aliphatic urea-diol chain extenders were synthesized from aliphatic diisocyanates (LDI or HDI) and AE at a molar ratio of 1:2. The reactions were carried out at 0°C with magnetic stirring and nitrogen flow. The absence of an isocyanate peak (2,250–2,280 cm^{-1}) in the Fourier transform infrared spectrum confirmed complete conversion, which yielded the chain extenders AE–L–AE and AE–H–AE, respectively. The aromatic diester-diphenol chain extender was synthesized by a Fisher esterification reaction between the carboxylic acid group of DAT and the hydroxyl groups of EG (DAT:EG molar ratio = 2:1), as showed in Scheme 1. The reaction was carried out in refluxing toluene in the presence of *p*-TsOH as Brønsted acid-catalyst to produce a diester-diphenol chain extender (D–E–D). The reaction was driven towards completion by using a Dean-Stark apparatus to trap the evolved water. Then, toluene was distilled off under vacuum. In order to remove any residual reactant, the product was washed twice with 50°C distilled water and filtered. Finally, the resulting white powder was dried under vacuum and stored in a desiccator until use. The reaction yield was 70%.

2.3 Synthesis of SPU series

SPU were obtained as previously described [24] with minor modifications. Briefly, PCL diol was reacted with HDI or LDI in a 1:2.01 molar ratio at 80°C in anhydrous DMAc under stirring and nitrogen atmosphere. The pre-polymerization proceeded in the presence of dibutyltin dilaurate as catalyst (0.1 wt.% of macrodiol) for 1 h, and then the solution was concentrated. The chain extenders AE–H–AE, AE–L–AE or D–E–D were previously dissolved in DMAc, and added at a molar ratio 1:1 with respect to the

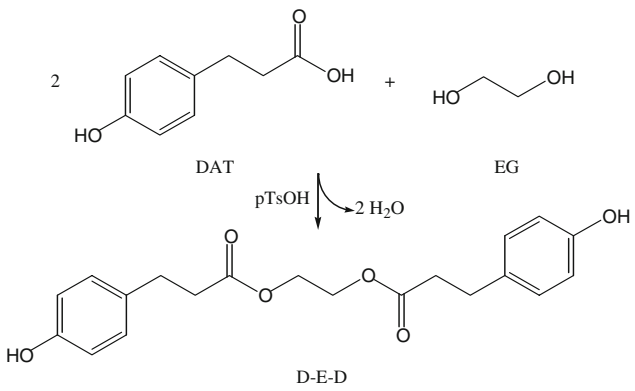

Scheme 1 Synthesis of D–E–D by esterification of DAT with EG

prepolymer. Chain extension reaction proceeded for 6 h at 80°C. The resulting slurry was precipitated over cold distilled water, except for D–E–D-extended SPU which were precipitated over ether. Then, polymers were washed and dried under vacuum. Films were prepared by solution casting from DMAc (10% w/v). SPU solutions were cast onto siliconized Petri dishes, the solvent was evaporated at 60°C, and finally dried under vacuum for 24 h. Polyurethane samples were designated as P*XY*, where P corresponds to PCL diol, *X* is the diisocyanate abbreviation, H or L (for HDI or LDI, respectively), and *Y* is the chain extender abbreviation: H, L or D (for AE–H–AE, AE–L–AE or D–E–D, respectively). SPU synthesized using HDI comprise the series H (PHH, PHL and PHD) whereas whose synthesized using LDI comprise the series L (PLH, PLL and PLD).

2.4 Physicochemical and mechanical characterization

Infrared analysis was performed using a Mattson Genesis II FTIR spectrometer at room temperature. Spectra of the monomers were obtained from KBr pellets. For SPU films, attenuated total internal reflectance (ATR-FTIR) spectra were obtained using the same spectrometer equipped with an ATR accessory. Spectra were collected from 64 scans at 2 cm^{-1} resolution. ^1H nuclear magnetic resonance (NMR) spectroscopy was performed using a Bruker AM-500 NMR spectrometer operating at 500 MHz. For chain extenders, all spectra were obtained at room temperature from 5% w/v DMSO-d_6 solutions, using a delay time between pulses of 5 seconds. Differential scanning calorimetry (DSC) was carried out in a Shimadzu DSC-50 calorimeter. Scans were performed at a heating rate of 10°C min^{-1}. Thermograms were obtained in the range −100°C to 250°C under nitrogen purge. The glass transition temperature (T_g) was taken at the onset of the transition. SPU molecular weights were estimated by intrinsic viscosity [η] measurements by means of an Ubbelohde Type OC viscosimeter (Cannon). The data were collected at 30 ± 0.1°C using DMAc as solvent.

Uniaxial tensile stress–strain data were obtained from an Instron model 4,467 testing machine. Sample strips of 35 × 5 × *t* (mm^3) (*t* = 0.3–0.5 mm) were cut from polymer films. Tests were performed using a crosshead speed of 5 mm min^{-1}, an extensometer for elastomers (Instron), and a loading cell of 100 N. At least four replicate measurements were taken and averaged. For determination of the tear strength, test trouser specimens 3.75 cm long, 1.25 cm wide with a longitudinal slit of 2.5 cm were used. The width of the tear path was 1.25 cm. During testing the force was applied normally to the plane, operating at a crosshead speed of 250 mm min^{-1} (ASTM D1938-02).

3 Results and discussion

3.1 Macrodiol and chain extenders characterization

PCL diol oligomers were constituted by two different types of TEG units: monosubstituted TEG species (HO–TEG–PCL–OH, 9.6%) and disubstituted TEG species (HO–PCL–TEG–PCL–OH, 90.4%). No free TEG species were found [24]. The chain length and relative amount of each species are not usually found in the literature. However this information results of significant importance as it indicates the uniformity of blocks that will form the soft segments in the polyurethane. FTIR showed the typical signals of an aliphatic polyester: 3,535 cm^{-1} (O–H groups), 2,945 cm^{-1} and 2,866 cm^{-1} (methylene groups), 1,723 cm^{-1} (carbonyl groups), 1,246 cm^{-1} and 1,194 cm^{-1} (C–O–C in ester groups). The thermal properties, measured by DSC, are shown in Table 1. The degree of crystallinity, calculated taking into account the melting enthalpy for 100% crystalline PCL (148.05 J g^{-1}) [25], was 65.5%.

The chemical structure of the synthesized urea-diol chain extenders, AE–H–AE and AE–L–AE, was determined by NMR spectroscopy, as described previously [24]. After a detailed analysis of the spectroscopic results, both diol chain extenders were completely characterized. AE–H–AE has a linear and symmetrical structure with two urea groups (Scheme 2a) whereas AE–L–AE presents an asymmetric structure composed of only one urea group and a heterocyclic-planar 3,5-disubstituted hydantoin (Scheme 2b). The chemical structure of diester-diphenol chain extender was also determined by NMR spectroscopy. The ^1H-NMR spectrum of D–E–D is shown in Fig. 1. The ratio of the area of peaks *d* and *e* (corresponding to methylene hydrogens of DAT) to that of peak *f* (methylene hydrogens of EG) was 2.03:1, which confirms that the reaction of the carboxylic acid group of DAT with the hydroxyl groups of EG forms a linear and symmetrical structure with two ester groups (Scheme 2c).

FTIR spectra of the three chain extenders are shown in Fig 2. The amine and carbonyl regions of the spectra provided information about the intermolecular attraction by hydrogen bonding (*H*-bonding). The AE–H–AE spectrum displayed a broad peak centered at 3,332 cm^{-1} (*H*-bonded

Table 1 Thermal properties of macrodiol and chain extenders measured by DSC

Macrodiol and chain extenders	T_g (°C)	T_m (°C)	ΔH_m (J g^{-1})
PCL diol	−69.3	50.5	96.9
AE–H–AE	–	193.6	210
AE–L–AE	–	118.8	150
D–E–D	–	120.9	140

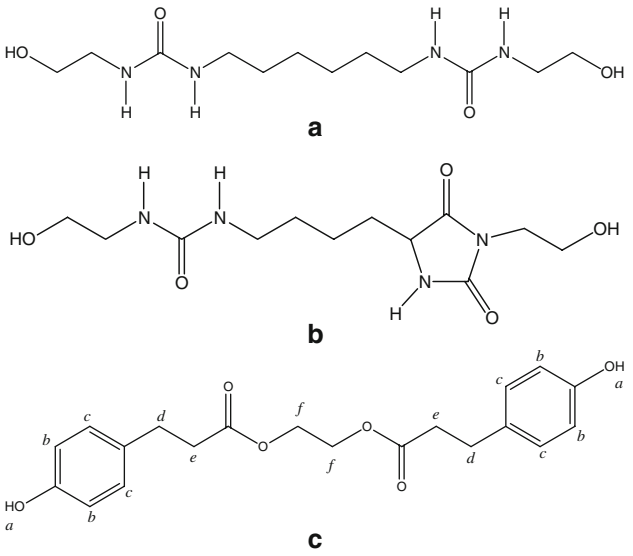

Scheme 2 Chemical structures of synthesized chain extenders: (**a**) AE–H–AE, (**b**) AE–L–AE, and (**c**) D–E–D showing in letters the proton NMR assignments

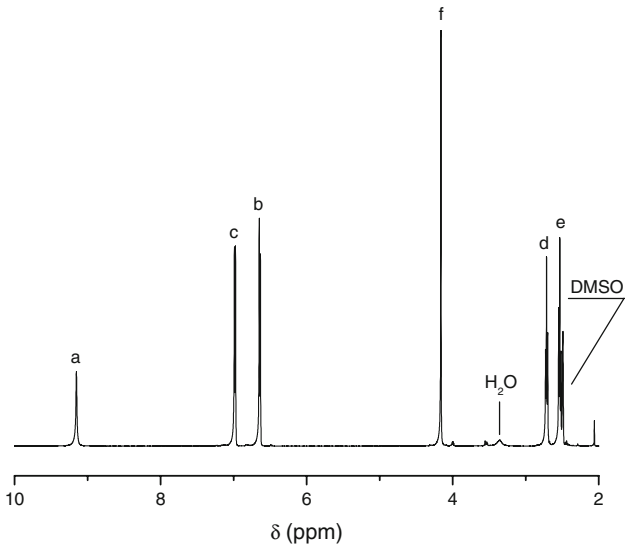

Fig. 1 ^{1}H-NMR spectrum of D–E–D chain extender

urea groups) and strong bands at 1,619 cm^{-1} (*H*-bonded carbonyl–urea amide I) and 1,588 cm^{-1} (urea amide II groups). No peak from free N–H groups could be seen (3,515 cm^{-1}). This is related to the high symmetry of the chemical structure and the presence of an even number of carbon atoms, which allowed a close chain association by hydrogen bonding. The spectrum of AE–L–AE exhibited peaks at 3,340 cm^{-1} (*H*-bonded N–H groups), 3,515 cm^{-1} (free N–H groups), 1,784 and 1,708 cm^{-1} (carbonyl groups of the hydantoin cycle), 1,622 and 1,586 cm^{-1} (ascribed to the same groups noted for AE–H–AE). The presence of non-bonded groups can be attributed to the asymmetric

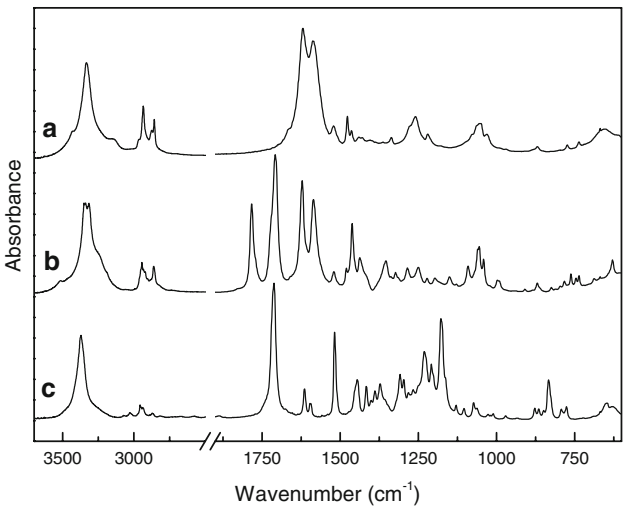

Fig. 2 FTIR spectra of synthesized chain extenders: (**a**) AE–H–AE, (**b**) AE–L–AE, and (**c**) D–E–D

structure of the chain extender, which inhibited the ordering and complete association of N–H groups. On the other hand, the aromatic chain extender, D–E–D, displayed signals at 3,371 cm^{-1} (O–H phenol group), 1,712 cm^{-1} (carbonyl ester groups), 1,614 cm^{-1} (C = C benzene ring), 1,518 cm^{-1} and 833 cm^{-1} (C–H in 1,4-disubstituted aromatic ring), 1,231 cm^{-1} (O–H and C–O phenol group), and 1,178 cm^{-1} (C–O ester group).

The thermal analysis showed that the three chain extenders were crystalline. The values of thermal properties are summarized in Table 1. The presence of two urea linkages and high structural symmetry in AE–H–AE chain extender led to a crystalline compound with high melting temperature. The thermal behavior of AE–L–AE was similar. The presence of an asymmetric structure containing a heterocycle did not hinder the formation of an ordered packing of molecules. The lower temperature is consistent with the presence of only one urea group by molecule, which provides lower cohesive forces. Despite the absence of N–H groups, D–E–D also exhibited crystallinity. The symmetric structure and the presence of aromatic rings in the chain extender led to a crystalline compound with values of the thermal properties close to the observed for AE–L–AE. All the chain extenders showed good solubility in DMAc and DMSO.

3.2 SPU synthesis and physicochemical characterization

Two series of PCL-based SPU were successfully synthesized and characterized in our laboratory (series H and L) incorporating three novel chain extenders AE–H–AE, AE–L–AE, and D–E–D. SPU were synthesized by a two-step polymerization method. At the first stage, PCL diol was

end-capped with either HDI or LDI to form the macrodiisocyanate. At the second stage, the chain extender was added to increase the molecular weight and promote microphase separation into a soft PCL-rich phase stabilized by van der Waals forces and a hard phase stabilized by *H*-bonding (SPU containing AE–H–AE and AE–L–AE) or by π-bond interactions (SPU containing D–E–D). The polymerization was performed at maximum concentration in a solvent in order to avoid concentration effects that could affect the molecular weight of the polymer. The reaction was stopped when complete disappearance of the isocyanate groups was observed by FTIR. The hard segment content of SPU were in the range of 21.8–25.9 wt.% (Table 2). The polymers obtained were non-sticky and slightly whitish.

The lower viscosity values for SPU series L with respect to the corresponding ones for SPU of series H (Table 2) can be explained by the difference in reactivity of the isocyanate groups in LDI. In HDI both isocyanate groups have the same reactivity, whereas in LDI the isocyanate group attached to the secondary carbon has a lower reactivity. This difference yielded asymmetric chemical structures in the hard segment borders in series L since LDI can react by means of two different coupling groups. In the case of HDI, the presence of groups with similar reactivity contributed to a better association degree of the hard segments, leading to higher viscosity values. The structure of the chain extender also determines the association degree of the hard segments. Therefore, the observed viscosity of SPU is related to both the isocyanate and the chain extender chemistry.

SPU could not be obtained following the methodology reported by Spaans et al. [26] where a long uniform-size diisocyanate block is reacted with the macrodiol. Chain extenders were reacted either with HDI or LDI to afford macrodiisocyanates (for example HDI–AE–H–AE–HDI). However, these pentablocks had a melting point above the decomposition temperature and were not soluble in any suitable solvent. The strong cohesion produced by the high density of *H*-bonding was responsible for this behavior.

When studying *H*-bonding by FTIR spectroscopy there are two major regions of interest: the N–H region found between 3,100 and 3,600 cm^{-1}, and the carbonyl region located between 1,600 and 1,800 cm^{-1}. FTIR spectra for the synthesized SPU are shown in Figs. 3 and 4. All the SPU samples exhibited signals corresponding to *H*-bonded groups, *H*-bonded urethane and urea (3,313–3,333 cm^{-1}) in AE–H–AE or AE–L–AE extended polymers or only *H*-bonded urethanes (3,368 cm^{-1}) in D–E–D extended polymers. The formation of carbonyl-urethane amide I groups (shoulder peak at 1,680–1,686 cm^{-1}) demonstrated the formation of urethane groups which connect soft to hard segments. Moreover, in AE–H–AE or AE–L–AE extended SPU, the signal at around 1,615–1,621 cm^{-1} was ascribed to *H*-bonded carbonyl-urea amide I whereas the signal at 1,579–1,589 cm^{-1} was attributed to stretching C–N plus bending N–H in carbonyl-urea amide II. Additionally, a peak corresponding to stretching C–N plus bending N–H in carbonyl-urea amide III (1,250–1,258 cm^{-1}) was also found. Amide II and III peaks were not detected for PLL sample.

3.3 Thermal properties

In SPU, phase separation of soft and hard segments can take place depending on their relative content, structural regularity and thermodynamic incompatibility. SPU thermal properties were analyzed by DSC and the results are summarized in Table 2. PHH showed a glass transition temperature of PCL soft segments ($T_{g,s}$) at −61.4°C. This value was very close to the measured for PHL and the lowest of all the observed in the obtained SPU. Moreover, the $T_{g,s}$ of AE–H–AE and AE–L–AE extended polyurethanes were lower than the reported ones in the literature for other PCL-based SPU [13]. The D–E–D extended polymers (PHD and PLD) showed $T_{g,s}$ around −53°C, indicating a certain degree of phase-mixed morphology.

Table 2 Hard segment content, intrinsic viscosity and thermal properties of synthesized SPU (Series H and L)

SPU Sample	HS content (%)[a]	[η] (dl g^{-1})	$T_{g,s}$ (°C)	$T_{m,s}$ (°C)	$\Delta H_{m,s}$ (J g^{-1})[b]	X_c (%)	$T_{g,h}$ (°C)	$T_{m,h}$ (°C)	$\Delta H_{m,h}$ (J g^{-1})[b]
PHH	21.8	0.40	−61.4	27.0, 39.9	31.5	27.2	108.2	162.2, 171.4	3.4
PHL	22.2	0.41	−61.1	29.0, 44.4	35.0	30.4	–	101.1	6.4
PHD	23.6	0.49	−53.2	26.6, 39.3	29.8	26.4	–	–	–
PLH	24.2	0.36	−59.5	29.6	29.1	25.9	65.6	160.6, 174.0	10.1
PLL	24.5	0.34	−58.9	36.0	50.0	44.7	–	82.0	3.2
PLD	25.9	0.46	−53.1	31.6	21.1	0.5	–	–	–

[a] Hard segment (HS) content is the weight percent of diisocyanate plus chain extender in the polymer calculated from the stoichiometry of the reaction

[b] Melting enthalpy expressed by weight of SPU

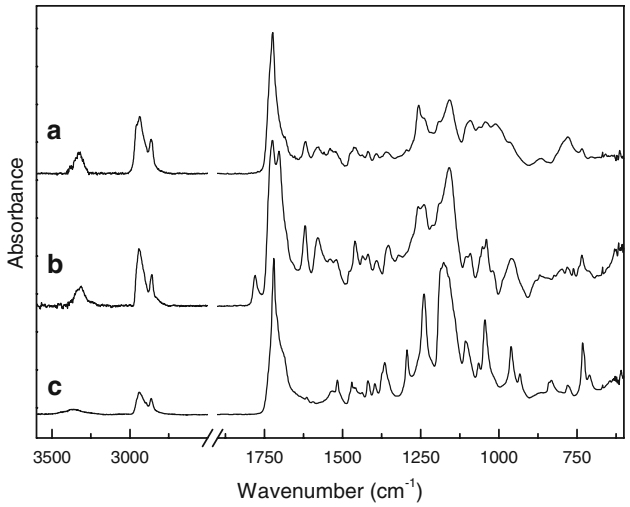

Fig. 3 ATR-FTIR spectra of SPU Series H: (**a**) PHH, (**b**) PHL, and (**c**) PHD

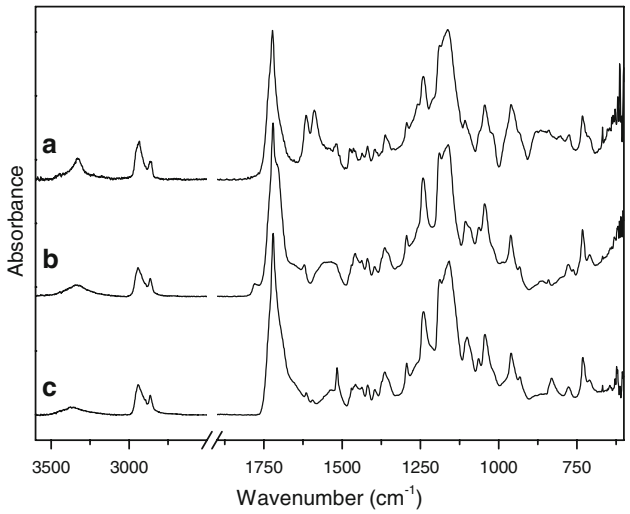

Fig. 4 ATR-FTIR spectra of SPU Series L: (**a**) PLH, (**b**) PLL, and (**c**) PLD

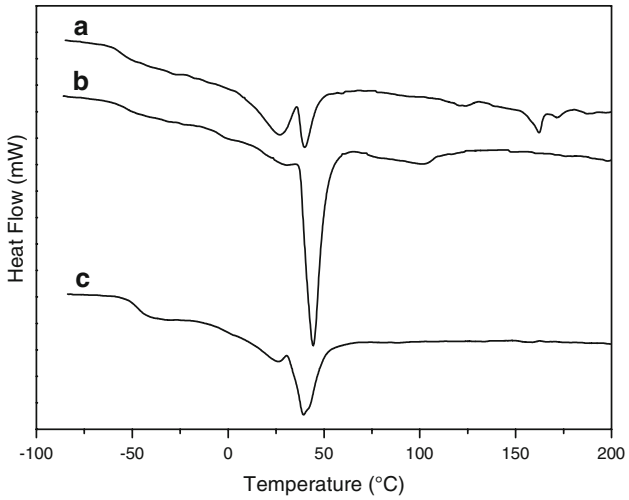

Fig. 5 DSC thermograms of SPU Series H: (**a**) PHH, (**b**) PHL, and (**c**) PHD

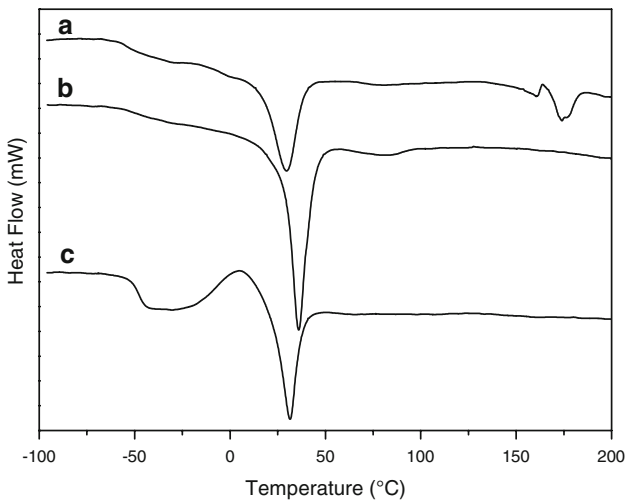

Fig. 6 DSC thermograms of SPU Series L: (**a**) PLH, (**b**) PLL, and (**c**) PLD

SPU series H displayed endothermal melting traces exhibiting two peaks ($T_{m,s}$) associated to soft segments (Fig. 5), whereas in series L only a single endotherm was observed (Fig. 6). In both series the $T_{m,s}$ values were lower than the melting temperature of PCL diol, as a consequence of the presence of less perfect crystals in the polymer compared to the PCL oligomer. The effect of connectivity between the hard and soft segments in crystallization emerged from melting enthalpies ($\Delta H_{m,s}$) analysis. A significant reduction in crystallinity (X_c) was observed for SPU samples, as previously suggested by the melting point. Only PLD was able to crystallize during the first DSC scan, displaying a broad exothermic crystallization peak (20.5 J g^{-1}) centered at 5.2°C. All the formed crystalline domains melted at 31.6°C, the original crystallinity being only 0.5%. At high temperatures in the series H, only PHH showed a second-order transition corresponding to $T_{g,h}$. A small exotherm was observed at 130.6°C followed by two endotherms at 162.2°C and 171.4°C. These transitions can be attributed to hard segment crystallization and melting of crystalline hard domains with different ordering degree, respectively. For PHH, the presence of structural symmetry and two urethane and two urea linkages into the hard segment led to hard segment association by *H*-bonding (Scheme 3a), which contributed to enhancing the phase separation. PHL also exhibited an endothermic peak at 101.1°C attributable to the melting of hard segments. In this case, the asymmetric structure of the chain extender did not avoid the hard segment association due to the possibility of *H*-bonding among urea, urethane and

carbonyl groups of hydantoin (Scheme 3b). As discussed before the asymmetric structure of AE–L–AE did not hinder the formation of an ordered packing. For PHD, thermal transitions of the hard segment were not detected by DSC.

Precedents in literature show that SPU based on PCL and LDI extended with lysine ethyl ester [5], phenylalanine or tyramine-based chain extenders [12, 20], did not show hard segment transitions except for one case where butanediamine chain extender was used [21]. In that reported SPU an endotherm centered at 90.9°C was assigned to melting of hard segments. However, the SPU samples PLH and PLL presented crystalline hard segment domains with some relevant differences. Although the two polymers had a lysine-derived joining block, PLL exhibited a very broad endotherm with low melting enthalpy whereas PLH had two sharp peaks with the higher hard segment melting enthalpy. For SPU series L, the composition and structure of AE–H–AE and AE–L–AE chain extenders had a significant effect in the hard segment chemistry. Despite the asymmetric structure of the LDI-capped prepolymer, the ability of AE–H–AE extended polymers to associate hard segment chains by *H*-bonding among symmetric chain extenders led to the formation of more packed hard domains. In the case of PLD, transitions corresponding to hard segments were not observed. This fact could be related to the presence of a more pronounced phase-mixed morphology, as it was mentioned before.

3.4 Mechanical properties

The results of the mechanical properties for the SPU samples are shown in Table 3. The Young's modulus (E), ultimate tensile stress (σ_u), ultimate strain (ε_u), yield stress (σ_y), yield strain (ε_y), and tearing energy (G_t) are listed for SPU series H and L. Fig. 7 shows the stress–strain curves for SPU series H. Two different behaviors were found in this series. On one side, PHH behaved as a soft elastomer, with lower Young's modulus and ultimate properties than PHL and PHD. Additionally, it was observed an increasing growth of stress with strain until chains became aligned and reached their maximum extension before breaking. There was no drawing of the polymer, and whitening due to strain-induced crystallization was not observed during tests. It is evident in this series that the chemical structure and symmetry of HDI and AE–H–AE chain extender enhanced the secondary bonding since the molecular chains are closely packed and parallel, increasing the ability of the hard segment to act as a physical crosslinking site (Scheme 3a). On the other side, PHL and PHD have a different hard segment structure (Scheme 3b and c), and behaved as tough plastics. These polymers displayed a yield point followed by necking, region where a very extensive reorganization of the polymer takes place. Once yielding was passed, stress dropped to a slightly lower value and then PHL exhibited plastic deformation by cold-drawing until a certain strain was reached. At this point, necking advanced through the entire specimen. At the end of this reorganization the curve changed the slope and the stress increased with strain until failure occurred. The region of cold-drawing was different in PHD, since the stress increased after yielding until necking was completed. PHD displayed higher ultimate strain (close to 1,000%) than PHL, the Young's modulus and ultimate stress being similar for both SPU. The combination of high tensile strength and high strain at break for PHD gives rise to an increase in the toughness, having PHD the highest of the series H, as determined by the area under the curve. In this case, the symmetric structure of HDI and D–E–D chain extender enhanced the secondary bonding within the hard segment (Scheme 3c), by *H*-bonding and π-stacking interactions, respectively.

SPU series L showed lower mechanical properties than the corresponding polymers in series H (insert in Fig. 7). PLH had half of the PHH Young's modulus value, whereas PLD displayed a modulus slightly lower than the measured for PHD. The structural differences between HDI and LDI revealed significant differences in both PHD and PLD polymers. The asymmetric structure of the reacted LDI in the border of the hard segment block hindered the formation of an ordered packing of hard segments. When strain at break values of PHD and PLD polymers were compared, a marked difference was found. The ultimate strain of PLD was reduced to only 7% (as can be clearly seen in the insert of Fig. 7). Following the same considerations about the chemical structure of lysine-derivative, as expected, PLL was a very weak polymer. Despite detecting hard segment melting traces by DSC, the asymmetry introduced in the hard segment by LDI and the lysine-based chain extender avoided the formation of extended and ordered regions. The low phase-separation degree noted in the series L had a significant impact in the resultant tensile properties. This phenomenon is believed to result from a decreased hard domain cohesion which produces a less phase segregated morphology [27].

Cyclic tensile tests carried out with increasing strain levels were performed on PHH and PHL samples and the results are shown in Fig. 8. PHH presented two characteristics of stress softening (Fig. 8a). First, upon subsequent straining, lower stress levels were observed for strain values lower than the previously applied; and second, at strain levels higher than those previously reached, the stress levels were apparently unaffected by prestraining. This stress-softening behaviour is characteristic of phase separated materials and several interpretations of the phenomena are cited in the literature [28, 29]. In a multiphase

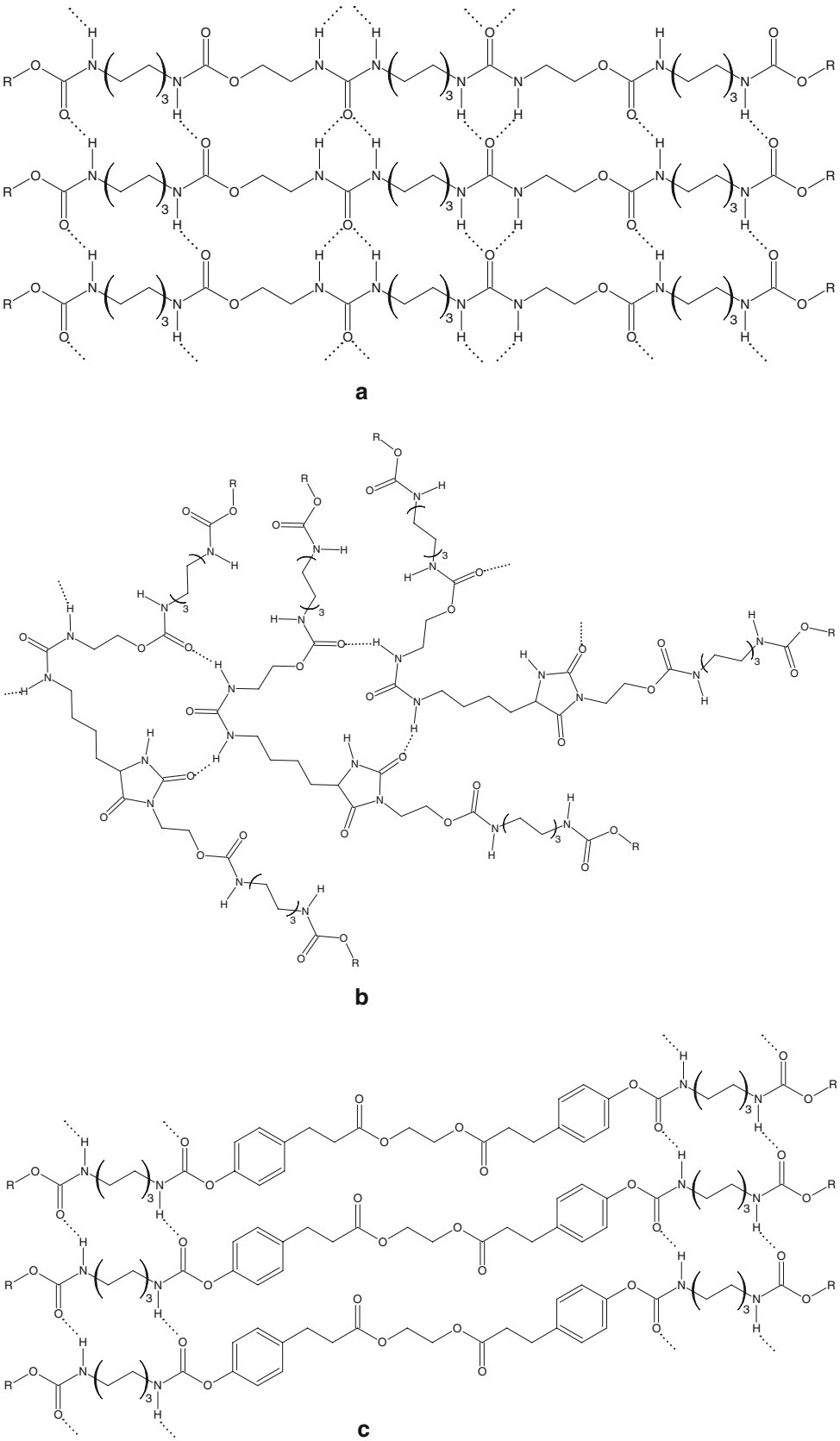

Scheme 3 Chemical structures proposed for the hard segment domains produced by *H*-bonding association in (**a**) PHH and (**b**) PHL, and *H*-bonding association plus π-stacking interactions in (**c**) PHD

Table 3 Mechanical Properties of SPU series H and L, as determined by uniaxial tensile testing

SPU	E (MPa)	σ_u (MPa)	ε_u (%)	σ_y (MPa)	ε_y (%)	G_t (kJ m^{-2})
PHH	16 ± 4	5.1 ± 0.3	469 ± 38	–	–	10.3
PHL	56 ± 3	7.0 ± 2.0	619 ± 155	5.2 ± 0.4	34 ± 8	8.9
PHD	54 ± 4	6.9 ± 1.5	1,006 ± 120	3.4 ± 0.9	19 ± 6	34
PLH	8 ± 2	1.1 ± 0.6	53 ± 18	–	–	6.5
PLL	4.7 ± 1.6	0.2 ± 0.1	8.7 ± 0.7	–	–	0.4
PLD	49 ± 3	2.2 ± 0.7	6.7 ± 1.4	–	–	3.0

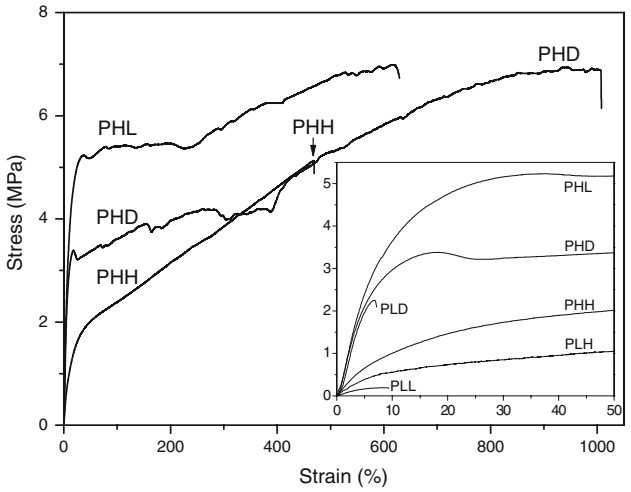

Fig. 7 Representative stress-strain tensile curves for SPU series H. Insert: Stress-strain curves for SPU series H and L in the region of low strain

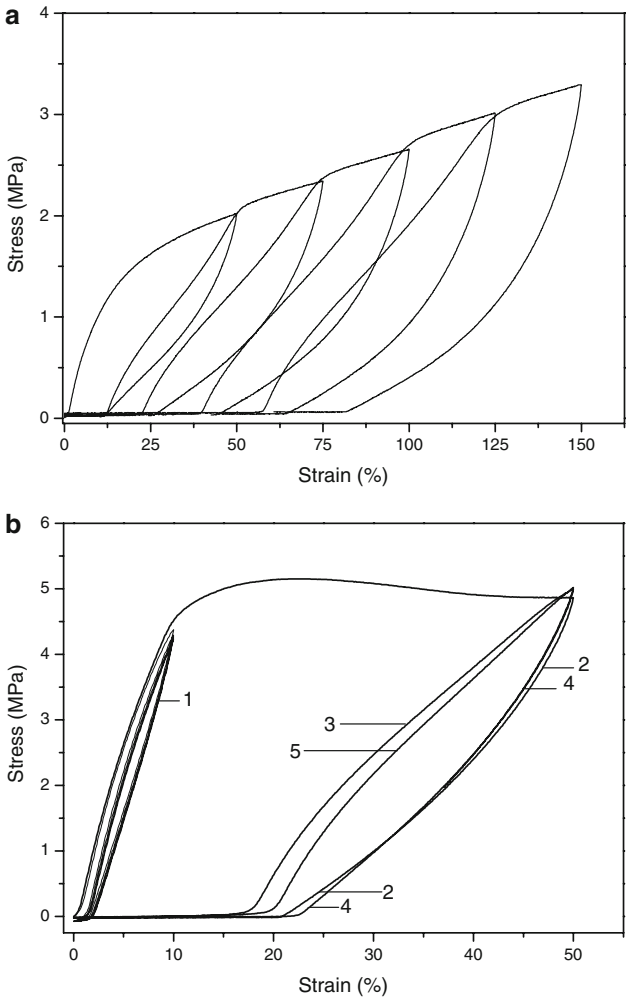

Fig. 8 Stress hysteresis versus strain for (**a**) PHH, and (**b**) PHL. The numbers in PHL curves indicate: (1) elastic region, (2) unloading after yielding, (3) loading second cycle, (4) unloading second cycle, and (5) loading third cycle

polymer, the hysteresis behavior is related to the morphology and composition of the phases [29]. The high hysteresis observed in PHH might be interpreted by the high hard segment interconnectivity which increases its plastic deformation upon strain. The stress disrupts ordering in hard domains, possibly leading to dissociation of some of the interurea *H*-bonding [30]. Figure 8b shows the hysteresis behavior of PHL polymers. Loading and unloading cycles were performed in the elastic region (1) and after yielding (2 to 5). In the elastic region, the observed hysteresis cycles were low. The repeated straining produced a small effect in the hysteresis behavior, the residual strain being almost constant. It is reasonable that no significant modification in the block copolymer structure is produced in the elastic region. Once yielding was passed, plastic deformation occurred and the hysteresis cycle and residual strain values were higher. As expected, the next cycles (loading curves 3 and 5) started from a prestrained sample. Taking this fact into account, for certain tissue engineering applications it is important to have high tensile stress at the yield point since inelastic deformations may cause catastrophic failure in a device, for example in the leaflets of a heart valve [19].

The tearing energy, determined as the tear strength (force applied over the thickness of the torn path) multiplied by two [31], is listed in Table 3. The G_t value of PHL was somewhat lower than the measured for PHH. This indicated that hard segments in PHL are less tight packed and then more easily disrupted than urethane-urea hard segments present in PHH. PHD showed the highest G_t

value. This can be explained by two processes that could occur to impede crack growth in PHD; less-cohesive hard domains can be more easily deformed and their morphology can change, which results in orientation. The tearing properties of SPU series L were poorer than the observed in series H samples. Again, the poor packing of the hard segments compared with the corresponding polymer of the series H, led to small resistance to tear.

As the mechanical properties strongly depend on the strain rate, temperature, and environmental conditions, these considerations should be carefully taken into account when comparing the observed stress-strain values with the reported ones for polymers with similar structure. From the previously discussed results, and considering the test conditions used in this work, the best mechanical properties were obtained for PHD.

Based on the obtained results and focusing on the application of the synthesized SPU in the soft tissue-engineering field, in vitro degradation behavior and processing into scaffolding materials are currently being investigated.

4 Conclusions

Two series of linear PCL-based SPU were successfully synthesized from either HDI or LDI and three novel chain extenders (two aliphatic urea-diols and one aromatic diester-diphenol) also prepared and characterized in author's laboratory. By varying the composition of the hard segment (diisocyanate and chain extender), the structure of the hard segment was varied to investigate the structure-property relationships. The different chemical structure and symmetry of hard segment modulated the phase separation of soft and hard domains, as demonstrated by the thermal behavior. Hard segment association was more enhanced using a combination of symmetric diisocyanate and urea-diol chain extenders (PHH and PHL). The hard segment cohesion had an important effect on the observed mechanical behavior. Polyurethanes synthesized using HDI were stronger than those obtained using LDI. Series L exhibited no tendency to undergo cold-drawing and the lowest ultimate properties. Incorporation of the aromatic chain extender produced opposite effects. In HDI-capped prepolymers resulted in polyurethanes (PHD) with the highest elongation and tearing energy. However the polyurethanes obtained from LDI-capped prepolymers and aromatic chain extender displayed a modulus slightly lower than PHD and the lowest strain at break (PLD).

The range of material properties that were achieved through minor modifications in the hard segment chemistry, as well as the use of non-toxic diisocyanate, makes these degradable polymers promising biomaterials for soft tissue-engineering applications. Studies on the biodegradation behavior and scaffold preparation are being carried out, and the results will be reported elsewhere.

Acknowledgements P.C. Caracciolo thanks to National Research Council (CONICET, Argentina) for the fellowship awarded. The authors would like to acknowledge the financial support of National Agency for the Promotion of Science and Technology (ANPCyT, Argentina), CONICET, and National University of Mar del Plata (Argentina).

References

1. G. Oertel, *Polyurethane Handbook* (Hanser Gardner Publications, Berlin, 1994)
2. P.A. Gunatillake, R. Adhikari, Eur. Cell. Mater. **5**, 1 (2003)
3. Gorna K, Gogolewski S in *Synthetic Bioabsorbable Polymers for Implants. ASTM STP 1396,* ed. by C.M. Agrawal, J.E. Parr, S.T. Lin (American Society for Testing and Materials, West Conshohocken, PA, 2000), p. 39
4. S.A. Guelcher, Tissue Eng. Part B **14**, 3 (2008)
5. A. Marcos-Fernández, G.A. Abraham, J.L. Valentín, J. San Román, Polymer (Guildf) **47**, 785 (2006). doi:10.1016/j.polymer.2005.12.007
6. C. Alperin, P.W. Zandstra, K.A. Woodhouse, Biomaterials **26**, 7377 (2005)
7. K.L. Fujimoto, J. Guan, H. Oshima, T. Sakai, W.R. Wagner, Thorac. Surg. **83**, 648 (2007). doi:10.1016/j.athoracsur.2006.06.085
8. J. Guan, K.L. Fujimoto, M.S. Sacks, W.R. Wagner, Biomaterials **26**, 3961 (2005). doi:10.1016/j.biomaterials.2004.10.018
9. K. Gisselfält, B. Edberg, P. Flodin, Biomacromolecules **3**, 951 (2002). doi:10.1021/bm025535u
10. R.G.J.C. Heijkants, R.V. van Calck, T.G. van Tienen, J.H. de Groot, P. Buma, A.J. Pennings, A.J. Pennings et al., Biomaterials **26**, 4219 (2005). doi:10.1016/j.biomaterials.2004.11.005
11. C.J. Spaans, J.H. de Groot, F.G. Dekens, A.J. Pennings, Polym. Bull. **41**, 131 (1998). doi:10.1007/s002890050343
12. S.A. Guelcher, K.M. Gallagher, J.E. Didier, D.B. Klinedinst, J.S. Doctor, A.S. Goldstein et al., Acta Biomater. **1**, 471 (2005). doi:10.1016/j.actbio.2005.02.007
13. K.D. Kavlock, T.W. Pechar, J.O. Hollinger, S.A. Guelcher, A.S. Goldstein, Acta Biomater. **3**, 475 (2007). doi:10.1016/j.actbio.2007.02.001
14. S.A. Riboldi, N. Sadr, L. Pigini, P. Neuenschwander, M. Simonet, P. Mognol et al., J. Biomed. Mater. Res. **84A**, 1094 (2008). doi:10.1002/jbm.a.31534
15. J.J. Stankus, J. Guan, K. Fujimoto, W.R. Wagner, Biomaterials **27**, 735 (2006). doi:10.1016/j.biomaterials.2005.06.020
16. M. Borkenhagen, R.C. Stoll, P. Neuenschwander, U.W. Suter, P. Aebischer, Biomaterials **19**, 2155 (1998). doi:10.1016/S0142-9612(98)00122-7
17. M.D. Lelah, S.L. Cooper, *Polyurethanes in Medicine* (CRC Press Inc, Boca Raton, Florida, 1986)
18. G.A. Skarja, K.A. Woodhouse, J. Biomater. Sci. Polym. Ed. **9**, 271 (1998). doi:10.1163/156856298X00659
19. Moore T, Ph.D. Thesis (Swinburne University of Technology, Australia, 2005)
20. J. Guan, M.S. Sacks, E.J. Beckman, W.R. Wagner, J. Biomed. Mater. Res. **61**, 493 (2002). doi:10.1002/jbm.10204
21. J.H. de Groot, R. de Vrijer, B.S. Wildeboer, C.J. Spaans, A.J. Pennings, Polym. Bull. **38**, 211 (1997). doi:10.1007/s002890050040

22. G.A. Abraham, A. Marcos-Fernández, J. San Román, J. Biomed. Mater. Res. **76A**, 729 (2006). doi:10.1002/jbm.a.30540
23. K. Gorna, S. Gogolewski, Polym. Deg. Stab. **75**, 113 (2002). doi:10.1016/S0141-3910(01)00210-5
24. P.C. Caracciolo, A.A.A. de Queiroz, O.Z. Higa, F. Buffa, G.A. Abraham, Acta Biomater. **4**, 976 (2008). doi:10.1016/j.actbio.2008.02.016
25. D.W. Van Krevelen, *Properties of Polymers* (Elsevier, Amsterdam, 1990), p. 121
26. C.J. Spaans, J.H. de Groot, V.W. Belgraver, A.J. Pennings, J. Mater. Sci. Mater. Med. **9**, 675 (1998). doi:10.1023/A:1008922128455
27. G.A. Skarja, K.A. Woodhouse, J. Appl. Polym. Sci. **75**, 1522 (2000)
28. G.M. Estes, S.L. Cooper, A.V. Tobolski, J. Macromol. Sci. Revs. Macromol. Chem. **C4**(2), 313 (1970)
29. J.A. Miller, S.B. Lin, K.K.S. Hwang, K.S. Wu, S.L. Cooper, Macromolecules **18**, 32 (1985). doi:10.1021/ma00143a005
30. T.D. Wang, D.J. Lyman, J. Polym. Sci. Polym. Chem. **31**, 1983 (1993). doi:10.1002/pola.1993.080310806
31. J.H. de Groot, R. de Vrijer, A.J. Pennings, J. Klompmaker, R.P.H. Veth, H.W.B. Jansen, Biomaterials **17**, 163 (1996). doi:10.1016/0142-9612(96)85761-9